

The 2002 June 22 Changureh (Avaj) earthquake in Qazvin province, northwest Iran: epicentral relocation, source parameters, surface deformation and geomorphology

Richard T. Walker,¹ Eric Bergman,² James Jackson,¹ Manoucher Ghorashi³ and Morteza Talebian^{1,3}

¹*Bullard Laboratories, Madingley Road, Cambridge CB3 0EZ, UK. E-mail: rwalker@esc.cam.ac.uk*

²*Department of Physics, University of Colorado at Boulder, Boulder, CO 80309–0390, USA.*

³*Geological Survey of Iran, Azadi Sq., Meraj Avenue, PO Box 13185–1494, Tehran, Iran*

Accepted 2004 October 25. Received 2004 September 18; in original form 2004 April 27

SUMMARY

The M_w 6.4 Changureh (Avaj) earthquake occurred on 2002 June 22, in Qazvin province, northwest Iran. We use observations from seismology, field investigation and analysis of satellite imagery and digital topography to suggest that slip on a previously unrecognized thrust fault (herein named the Abdarreh fault) was responsible for the earthquake. Inversion of long-period P and SH body wave seismograms shows rupture on a thrust fault dipping 49° to the southwest and with a centroid depth of ~ 10 km. Multiple-event relocation of the main shock and aftershock epicentres and discontinuous surface ruptures observed after the earthquake are compatible with a northwest-propagating rupture on a southwest-dipping thrust, but maximum recorded displacements are much less than expected from seismology, suggesting that much of the slip failed to reach the surface and was accommodated as folding at the surface instead. Long-term folding is difficult to see in the topography of the epicentral region as the Abdarreh fold is growing through a relict Neogene topography. Anticlinal uplift can, however, be inferred from drainage disruption and stream incision. The 2002 June 22 Changureh earthquake shows the importance of being able to interpret diagnostic features of active faulting in the landscape.

Key words: Changureh (Avaj) earthquake, earthquake location, geomorphology, Iran, seismology, thrust faulting.

1 INTRODUCTION

The M_w 6.4 Changureh (or Avaj) earthquake occurred at 07:28 local time (02:58 GMT) on 2002 June 22, in a sparsely populated region of Qazvin province in northwest Iran (Fig. 1). Despite the low population density, the earthquake caused widespread destruction, killing 261 people and injuring a further 1300 people.

Although destructive earthquakes have occurred before in Qazvin province, such as the 1962 September 1 Buyin Zahra earthquake (Fig. 1; Ambraseys 1963; Berberian 1976; Ambraseys & Melville 1982), no active faults had previously been mapped in the epicentral region of the Changureh earthquake (Blourchi & Hajian 1979). In this paper we show, nonetheless, that subtle surface indications of active faulting can be seen in the local geomorphology. We use a multiple-event relocation method to determine the epicentral location of the Changureh earthquake, and body wave seismology to determine the source parameters of the earthquake, which are consistent with northwest-propagating rupture on a thrust fault at depth, expressed at the surface predominantly as co-seismic anticlinal folding in alluvium. We call this previously unknown system the Abdarreh thrust fault.

Thrust faults that are not expressed as discrete scarps at the surface (known as ‘blind’ faults) are a problem encountered in many seismically active regions, and blind faults have been responsible for many destructive earthquakes in Iran and elsewhere. Although the surface deformation created by blind thrust earthquakes is in the form of anticlinal folding (e.g. Stein & Yeats 1989; Parsons *et al.* 2005), the surface expression of long-term folding from many repeated earthquakes is not always easy to see in the landscape, as the relatively small amounts of uplift involved in anticlinal folding are easily masked by pre-existing topography and geology. We show that although the fault responsible for the 2002 Changureh earthquake is hard to identify from topography alone, long-term fold uplift can be inferred from the patterns of drainage and stream incision.

2 GEOLOGICAL AND TECTONIC SETTING

The active tectonics of Iran is dominated by the northward motion of Arabia with respect to Eurasia (Fig. 1). At longitude 49°E , ~ 20 mm yr^{-1} of north–south shortening is accommodated across

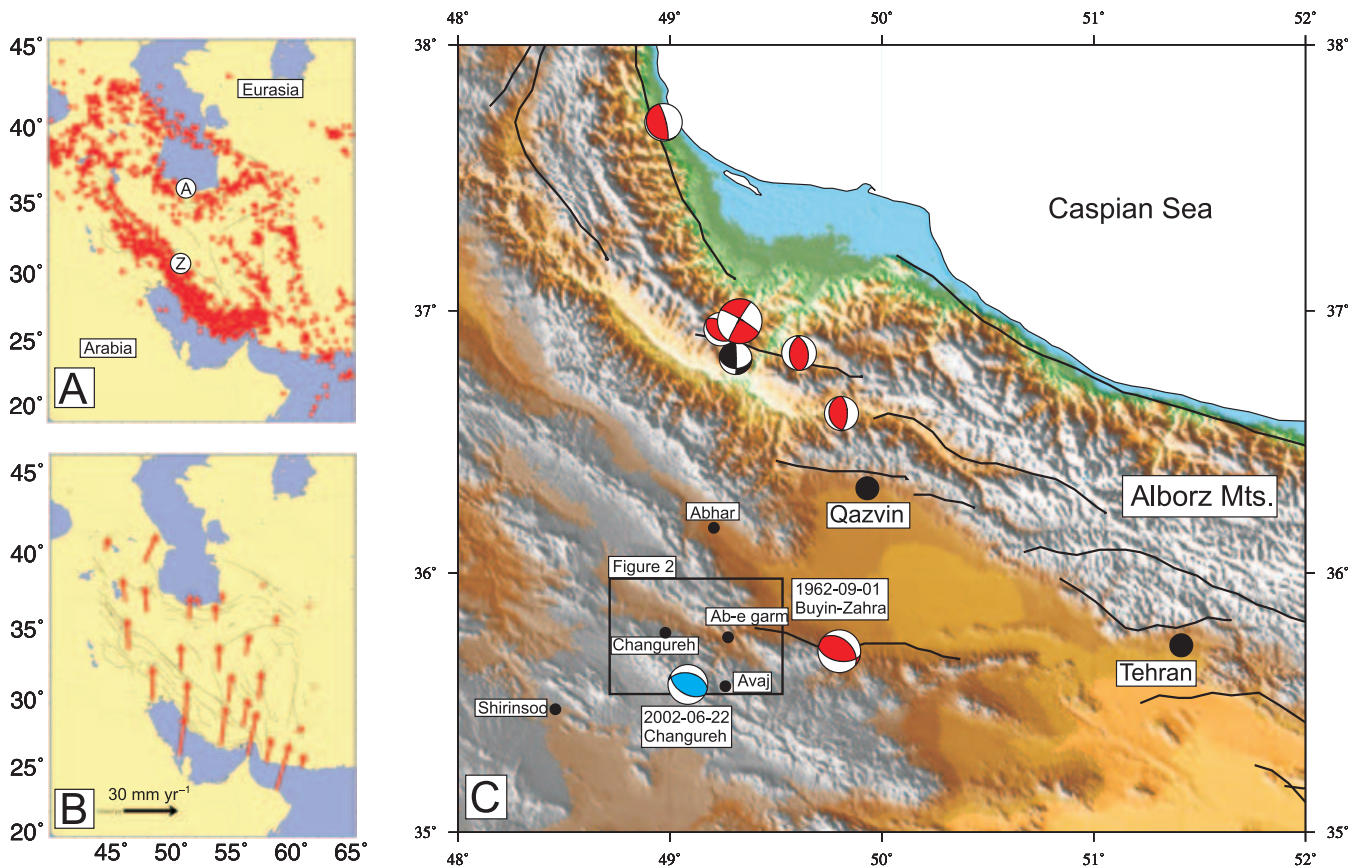


Figure 1. (a) Earthquake epicentres in Iran from the catalogue of Engdahl *et al.* (1998). Deformation is concentrated in the Zagros mountains (Z) in the south and the Alborz mountains (A) in the north. (b) A velocity field for Iran determined from repeated GPS measurements (Vernant *et al.* 2004). (c) Topographic map of known active faults (from Berberian & Yeats 1999) and earthquake fault-plane solutions in northwest Iran. The fault-plane solution of the 2002 June 22 Changureh earthquake is drawn in blue. Other fault-plane solutions are from Jackson (2001). The box shows the region represented in Fig. 2.

Iran (Sella *et al.* 2002; McClusky *et al.* 2000; Vernant *et al.* 2004), of which roughly half is accommodated in the Zagros mountains in the south of the country (Tatar *et al.* 2003), while the remainder is taken up in the Alborz mountains and South Caspian Basin to the north (Fig. 1; Jackson *et al.* 2002; Vernant *et al.* 2004). The 2002 Changureh earthquake occurred in a zone of active thrust faulting and folding parallel to, but south of, the southern margin of the Alborz mountain range (Fig. 1). This belt has generated several destructive 20th century and historical earthquakes, including the 1953 Torud earthquake and the 1962 Buyin Zahra earthquakes, 50 km to the east of the 2002 Changureh event (e.g. Ambraseys & Melville 1982).

The 2002 epicentral region lies within the Khar river valley (Figs 2 and 3). To the north, the valley is bounded by the northwest–southeast trending Kuh-e-Shah Golak mountain range (elevations up to 2898 m), which expose a sequence of Triassic and Jurassic metamorphosed limestones. To the south, the river valley is bounded by exposures of Mesozoic and Late Tertiary volcanic and sedimentary rocks of the Kuh-e-Yumer Qezel mountains (with elevations of up to 2540 m). The Avaj fault zone runs along the northern margin of the Kuh-e-Yumer Qezel mountains and is a major structure that controlled facies distribution throughout the Mesozoic and Late Tertiary. It separates the distinct lithological and structural history of the Razan structural zone in the south from that of the Ab-e-Garm zone in the north (Fig. 2; Blourchi & Hajian 1979).

A folded sequence of Miocene sandstones and marls (the Avaj red beds) is exposed within the Khar river valley (Fig. 2). The Miocene

red beds outcrop in several places in the Khar river valley as flat-topped outliers (Fig. 3). River and alluvial gravels are exposed extensively throughout the valley.

3 THE 2002 JUNE 22 CHANGUREH EARTHQUAKE (M W 6.4)

3.1 Overview and macroseismic effects

The 2002 June 22 Changureh earthquake occurred at 07:28 local time (02:58 GMT). The epicentre relocated by E. R. Engdahl (personal communication, University of Colorado, Boulder), using the Engdahl *et al.* (1998) algorithm, is at 35.572°N, 49.085°E (Fig. 2). Teleseismic locations in Iran may be in error by at least 10 km (Berberian 1979a; Ambraseys 2001). Multiple-event relocation of epicentres in the Changureh region (described in detail in Section 3.2), yields an epicentre for the 2002 June 22 main shock which is shifted ~10 km northeast from the initial position to an absolute location of 35.636°N, 49.199°E (see Table 1 and Fig. 2). This location is to the south of the Khar river valley, at the margin of the Kuh-e-Yumer Qezel mountains (Fig. 2). Several aftershocks and two earlier events were recorded teleseismically (see Table 1). The shifted relocations of these events (determined using the method described in Section 3.2) are shown as blue circles on Fig. 2.

The greatest damage occurred in the villages of Changureh and Abdarreh (Figs 2, 3 and 4), where almost all buildings were

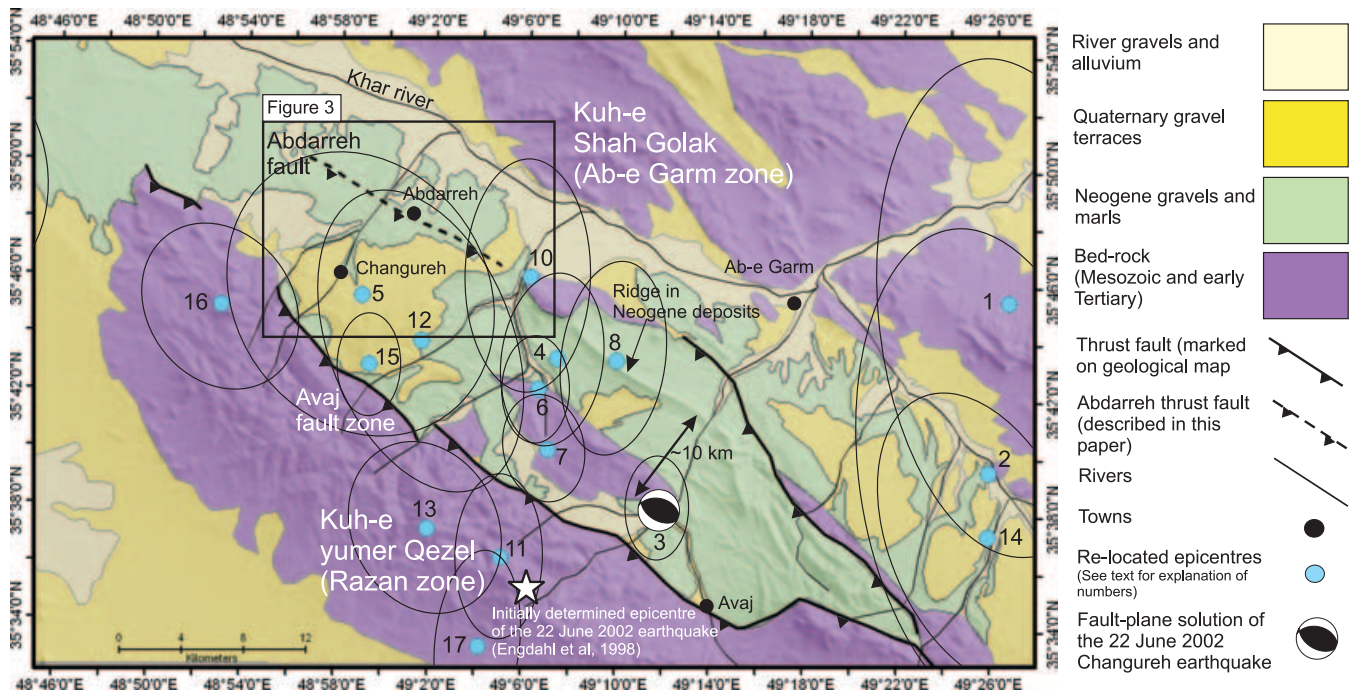


Figure 2. Geological map of the Changureh region (adapted from Blourchi & Hajian 1979). South of the Avaj fault zone, Mesozoic and early Tertiary bed rock in the Kuh-e-Qumer Yezel mountains belongs to the Razan group, which is a Zagros assemblage. Rocks within the Kuh-e-Shah Golak mountains belong to the Ab-e-Garm group, which is typical of Central Iran. Neogene conglomerates, sandstones and marls are exposed across much of the region, but are covered in places by Quaternary gravel terraces and younger alluvium in the river valleys. The Abdarreh fault is included here, but was not marked on the original map of Blourchi and Hajian (1979). The white star represents the teleseismic epicentre of the 2002 June 22 Changureh earthquake (E. R. Engdahl, personal communication, University of Colorado, Boulder, following the method of Engdahl *et al.* 1998). The fault-plane solution of the 2002 June 22 Changureh earthquake showing source parameters determined by long-period body wave modelling (see Table 2 and Fig. 6) is placed at the epicentre corrected from the teleseismic epicentre with respect to a locally recorded aftershock (see Section 3.2 for a full description of the method). Numbered blue circles represent the absolute epicentres of other teleseismically recorded earthquakes in the region. Ninety per cent confidence ellipses are plotted. Event numbers refer to entries in Table 1. (Note that event number 9 in Table 1 is located outside the boundary of this figure.) The box indicates the region represented in Fig. 3.

Table 1. Epicentres of earthquakes in the Changureh region. Origin times and locations reflect correction for teleseismic location bias using the local network solution for the 2002.07.03 event (see text). *N* is the number of readings used for the estimation of relative location. A1 and A2 are the azimuths in degrees, clockwise from north, of the semi-axes of the 90 per cent confidence ellipse for relative location. L1 and L2 are the corresponding semi-axis lengths in km. Area is the area in km² of the 90 per cent confidence ellipse.

Event	Date	Time (GMT)	Lat.	Lon.	Dep.	Mag.	N	A1	L1	A2	L2	Area
1	1967.08.25	12:26:44.65	35.758	49.444	8.0	4.7	19	83	8.2	173	16.1	415
2	1984.09.09	17:54:55.34	35.659	49.431	8.0	4.6	18	81	8.2	171	16.0	413
3	2002.06.22	02:58:20.07	35.636	49.199	10.0	6.2	264	84	1.9	174	3.3	20
4	2002.06.22	03:31:55.40	35.722	49.123	8.0	4.4	57	271	3.1	1	5.7	56
5	2002.06.22	04:33:27.16	35.757	48.983	8.0	4.1	11	56	8.1	146	9.6	243
6	2002.06.22	06:45:33.46	35.704	49.110	8.0	4.9	176	271	2.1	1	3.5	24
7	2002.06.22	14:27:15.79	35.669	49.117	8.0	4.5	86	78	2.5	168	3.4	27
8	2002.06.22	21:33:25.09	35.721	49.165	8.0	4.5	54	275	3.3	5	6.4	66
9	2002.06.24	13:21:19.11	35.824	48.700	8.0	4.3	15	82	5.2	172	7.4	120
10	2002.06.24	21:30:39.22	35.769	49.103	8.0	4.4	20	273	4.0	3	7.6	97
11	2002.06.26	18:18:13.65	35.606	49.085	8.0	4.6	45	272	2.8	2	5.3	46
12	2002.07.03	19:24:39.20	35.731	49.026	7.4	4.3	11	68	5.8	158	10.2	188
13	2002.07.25	13:29:56.82	35.622	49.032	8.0	4.5	25	64	4.7	154	5.7	85
14	2002.08.23	13:04:59.90	35.622	49.431	8.0	4.3	12	67	6.0	157	10.0	188
15	2002.09.02	01:00:02.13	35.717	48.989	8.0	5.1	208	85	2.0	175	3.4	22
16	2002.09.02	16:34:18.96	35.750	48.883	8.0	4.2	17	58	4.7	148	5.8	86
17	2002.11.07	16:42:10.23	35.554	49.070	8.0	4.8	36	274	2.7	4	6.1	52

destroyed (Figs 4a and b). These villages are located ~25 km from the epicentre of the main shock (Fig. 2). Lesser damage was more widespread, but all structural damage was confined within a region bounded by Avaj in the south, Ab-e-Garm in the east, Shirinsoo in

the west and Abhar in the north (Fig. 1c). The relatively high levels of damage at Changureh and Abdarreh in comparison to Avaj and Ab-e-Garm would suggest focusing of damage to the northwest of the epicentre, presumably due to northwestward rupture

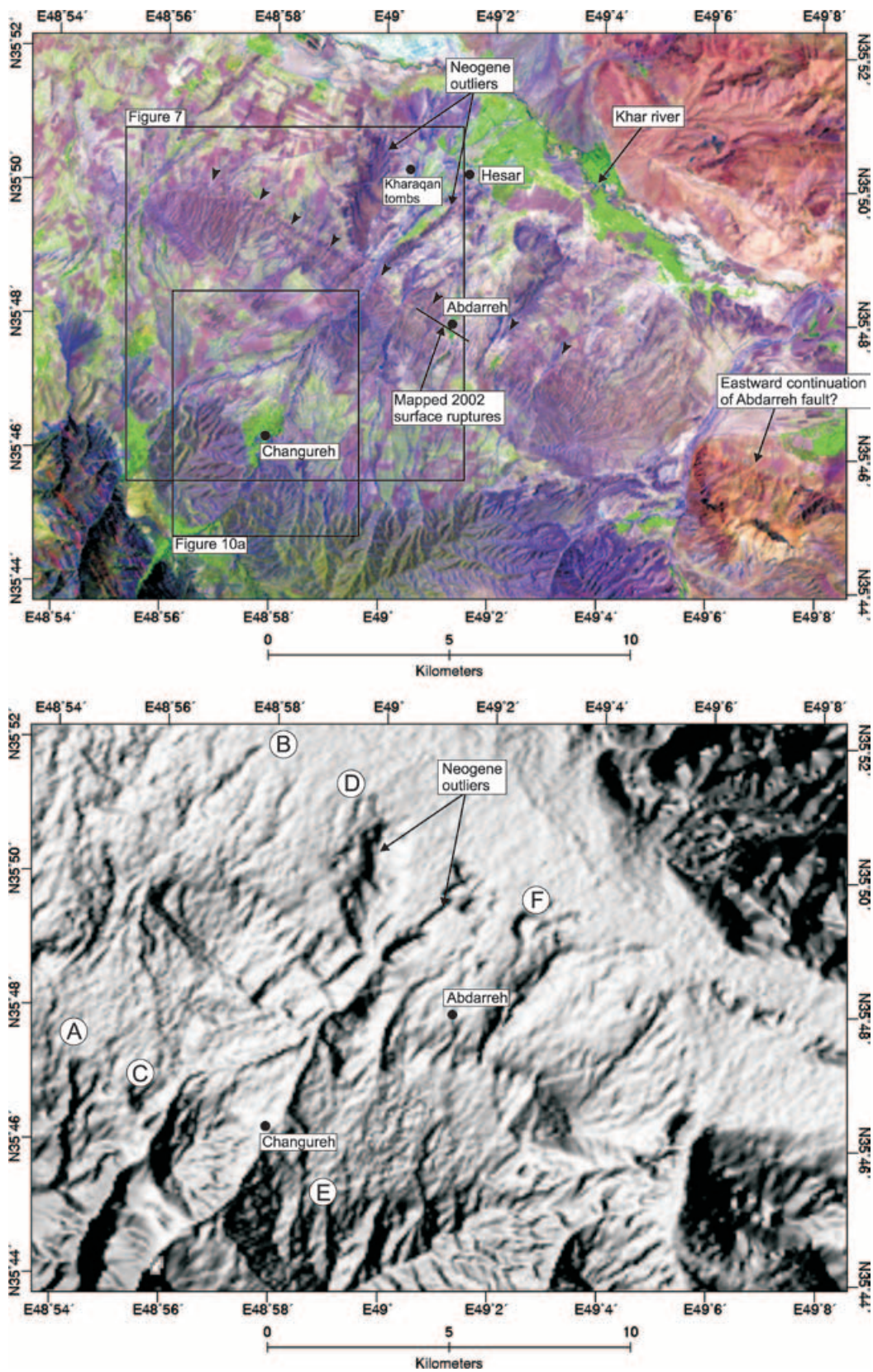


Figure 3. (a) LANDSAT TM+ satellite image (RGB bands 5,4,1) of the Changureh region. The wide, low-relief Khar river valley occupies much of the scene. Remnants of a resistant Neogene gravel surface crop out within the valley. A sharp break in fluvial incision is marked by black arrows. This break is inferred to be the surface expression of the northwest–southeast-trending Abdarreh thrust fault. Surface ruptures initially reported by IIEES and GSI after the 2002 Changureh earthquake are marked as a black line. (b) SRTM digital elevation model of the Changureh region (illuminated from the southeast). Circled letters mark the lines of section in Fig. 9.



Figure 4. (a) Photograph looking roughly north from $35^{\circ}47'41.5''\text{N}$, $49^{\circ}07'22.9''\text{E}$ at earthquake damage at Abdarreh. (b) Close-up of earthquake damage to single-storied adobe housing at Abdarreh. (c) Kharaqan Seljuk domed mausoleum near Hesar ($35^{\circ}50'27''\text{N}$, $48^{\circ}57'40''\text{E}$, see Fig. 3 for location), damaged during the 2002 Changureh earthquake. (d) Thrust ruptures observed near Abdarreh village at $35^{\circ}47'41.5''\text{N}$, $49^{\circ}07'22.9''\text{E}$.

propagation see also Section 4.2). The majority of structural damage was caused by failure within single-storey adobe buildings (e.g. Figs 4a and b).

The earthquake also damaged the Kharaqan tomb towers, which are important historical monuments in the area (Fig. 4c). This pair of domed Seljuk tombs are situated ~ 2 km west of Hesar (Fig. 3), and date from AD1067–8 and AD1093 (Matheson 1976). In the absence of recorded historical earthquakes (e.g. Ambraseys & Melville 1982), the good state of preservation of these monuments prior to 2002 suggests that the Changureh earthquake was the first large event to strike this region for over 900 yr.

3.2 Relocation of Changureh epicentres

We relocated the Changureh main shock, aftershocks, and several earlier events with a recently developed technique that yields improved accuracy for both the relative and absolute locations of clustered earthquakes. We use a multiple-event relocation method with regional and teleseismic phase arrival times to constrain relative locations of clustered earthquakes. We then calibrate the absolute location of the cluster by obtaining independent information on the absolute location of one or more members of the cluster. For

the multiple event relocation (cluster analysis) we use a version of the hypocentroidal decomposition (HDC) method first proposed by Jordan & Sverdrup (1981), which has been developed specifically for this kind of ‘ground truth’ research. Further explanation of the methodology may be found in Ritzwoller *et al.* (2003) and Bondar *et al.* (2004). In the case of the Changureh cluster we obtained an accurate location of one of the cluster events from an aftershock study, using data completely independent of those used in the HDC analysis. We note that double-difference and master event methods are also sometimes used to relocate spatially clustered earthquake events (e.g. Zhou 1994; Mori *et al.* 1995; Waldhouser & Ellsworth 2000; Shearer 2002). However, a full discussion of these other methods is beyond the scope of this paper.

The cluster of earthquakes used in the analysis was extracted from a recently compiled database of well-constrained earthquakes in the Iran region (E. R. Engdahl, personal communication, University of Colorado, Boulder). The events are carefully relocated in a single-event code based on the algorithm of Engdahl *et al.* (1998) in which considerable care goes into proper phase identification, flagging of outliers (readings with relatively large residuals against a reference traveltimes model) and analysis of open azimuth. For multiple-event relocation it is necessary to keep the dimensions of the cluster small

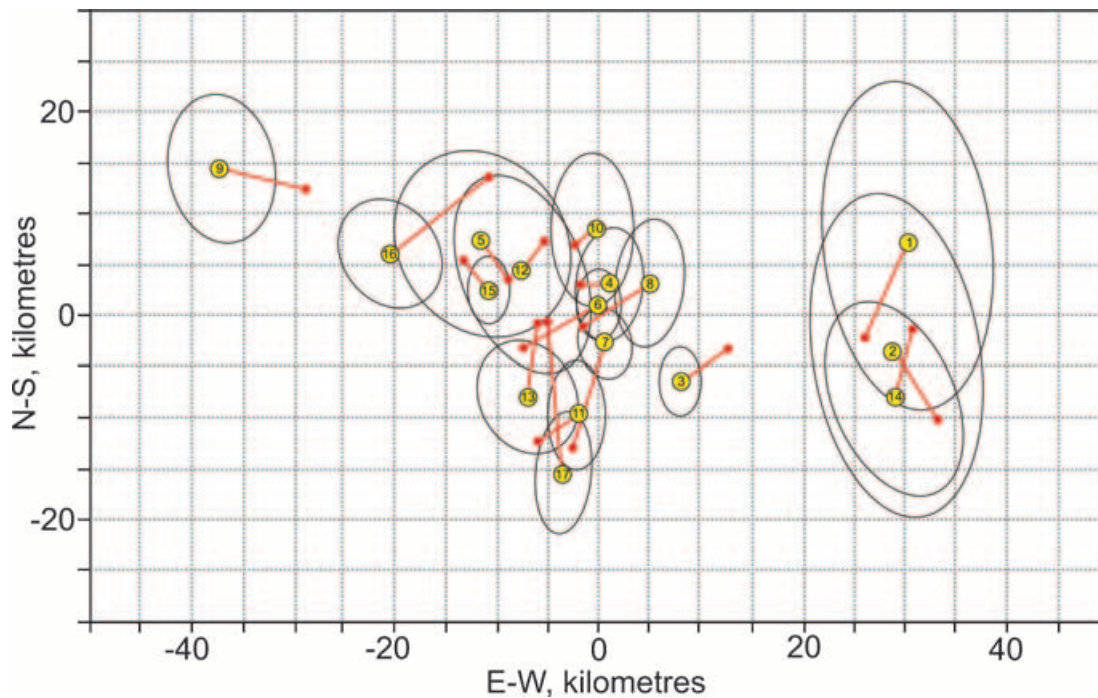


Figure 5. Locations of earthquakes in the Changureh region relative to the hypocentroid (or geometrical) centre of the cluster vectors. Relative locations of clustered events are determined using the hypocentroidal decomposition (HDC) method of Jordan & Sverdrup (1981). Ellipses represent the 90 per cent confidence limit on the locations. Events are numbered as in Table 1. Red lines connecting to the centre of the ellipses indicate the change in position between the initial single event (represented by red dots) and the multiple event locations relative to the hypocentroid of the clustered events. For example, after HDC analysis, the location of the main shock (event number 3) is shifted from its initial position by 5.3 km at an azimuth of 236° relative to the hypocentroid of the cluster. Note that the absolute relocations shown in Fig. 2 involve a further shift of the clustered events shown here, such that the position of event 12 coincides with the hypocentre determined from an independent local network (see text for further details).

enough (typically 50–75 km across) to avoid the effects of significant lateral heterogeneity in the crust and upper mantle. We started by examining all events with single-event solutions within about 50 km of the Changureh main shock. Outlying events were discarded. Taking events with single-event solutions within about 30 km of the Changureh main shock, we formed a cluster of 17 events (Table 1) for HDC analysis.

The data sets of regional and teleseismic phase arrival times for these events are dominated by first-arriving P_n and P phases, but we use other phases when they are available. S_n phases are sometimes quite important for constraining relative locations because of their low apparent phase velocity.

Because there is little constraint on source depth from regional and teleseismic phases (there are no reliable depth phases reported for these shallow events), we fixed the depths of all events for the HDC analysis. The main shock was set at 10 km, based on body waveform modelling (see Section 3.4 and Fig. 6) and we set the depth of event number 12 at 7.4 km based on our relocation of this event using arrival times from a local network aftershock study (provided by A. M. Farahbod, personal communication, IIEES, Tehran). Our relocation of event 12 is described later in this section. The remaining events were set at 8 km. Errors of 5 km or more in assumed depth have little impact on estimates of the epicentres, but there is a well-known trade-off with origin time.

During the HDC analysis we perform additional ‘cleaning’ of outlier phase readings, taking advantage of the redundancy of readings at a given station that observed several cluster events. Consideration of the pattern of residuals (for a given phase) for all cluster events observed at a station also allows us to make an empirical estimate

of the average reading error at that station for this cluster. We make an estimate of the spread of residuals for this purpose. This is a significant improvement over standard single-event location algorithms which are forced to assume an *a priori* value for reading error which is applied to all stations and phases. Empirical weighting of the phase arrival data redistributes data importance in the inversion and leads to more accurate estimates of relative locations. It allows us to utilize different phases with very different reading errors. A second advantage is that as they are based on our estimates of average reading error for each station, the confidence ellipses on the relative locations derived from the inversion are more statistically valid.

The result of our HDC analysis of the Changureh earthquakes is shown in Fig. 5, which shows the relative locations of events with respect to the hypocentroid or geometrical centre of the cluster vectors that describe the relative locations. Ellipses are 90 per cent confidence limits. Events are numbered as in Table 1. The line connecting to the centre of each ellipse indicates the change in relative location from the starting locations (from single-event location).

The Changureh main shock (event number 3 in Fig. 2 and Table 1) is isolated from the other earthquakes. Most of the aftershocks occur to the northwest of the main shock. Event 9 may be as much as 50 km from the main shock, but it is located with only 15 phase readings and is susceptible to bias from one or a few outlier readings that may dominate the solution. There were a number of flagged outliers that suggest there may have been two events close in time that have been associated as one. We do not put great confidence on the location for event number 9. Event 14 is located 20 km east of the main shock, and although the quality of the location itself is not high it

22 June 2002 Changureh/Avaj 120/49/101/10/5.6E18

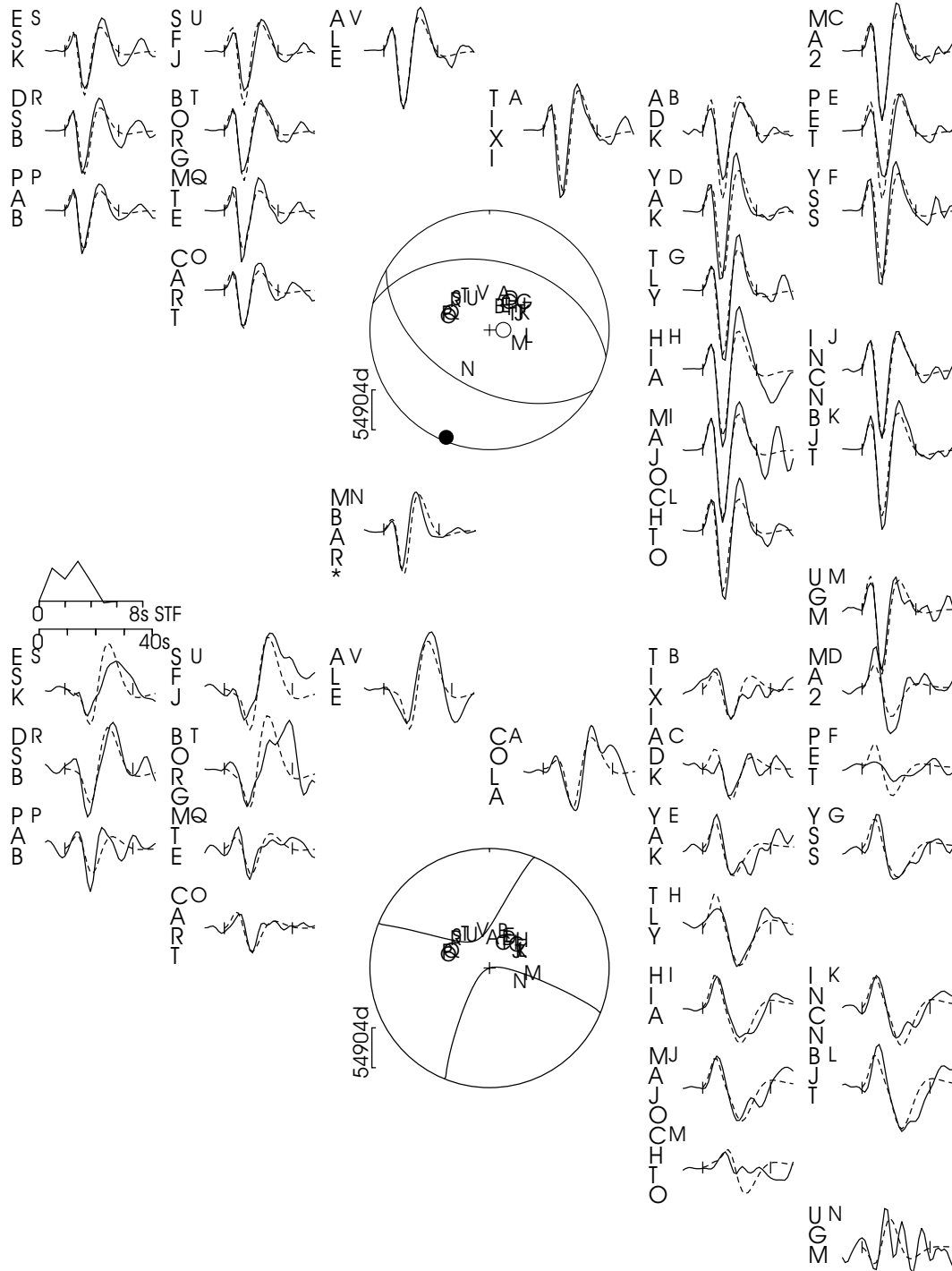


Figure 6. Minimum misfit solution for the 2002 June 22 Changureh earthquake. The top hemisphere represents the *P* wave radiation. The bottom hemisphere represents the *SH* waveforms. Station positions on the focal spheres are identified by capital letters and arranged clockwise from north. Waveforms for each station (identified by a three- or four-letter code, and a capital letter corresponding to those within the focal spheres) are positioned azimuthally around the focal spheres. Observed waveforms are shown as solid lines and synthetic waveforms as dashed lines. Numbers beneath the header line are strike (error $\sim 10^\circ$), dip (error $\sim 5^\circ$), rake (error $\sim 10^\circ$), centroid depth (in km, with an error of ± 3 km) and moment (in N m). The source–time function and waveform timescale are plotted between the two focal spheres. The synthetics are calculated for a layer 5 km thick with V_p 6.0 over a half-space of V_p 6.8. At station MBAR the gain was evidently wrong by a factor of 5. This has been corrected, but the station was not used in the inversion.

is co-located with two earlier events included in the cluster (from 1967 and 1984, events number 1 and 2 in Table 1). We therefore suspect that there is a zone of diffuse seismicity in the area east of Ab-e-Garm (Fig. 2) that was reactivated by the Changureh main shock.

Three aftershocks (11, 13 and 17) locate directly west of the main shock by 10–15 km. All the smaller events in this cluster suffer from poor data coverage to the south which increases the chance of the relative location being biased in latitude. If there are a significant number of late readings (very common for small events) at northern azimuths the effect will be to push the locations to the south. Because there are three such events close together, we believe these locations may be valid, and represent a secondary locus of aftershock activity. It would be unwise to assign much significance to this observation, however. The most robust conclusion of the HDC analysis is that the aftershock activity was dominantly to the northwest of the epicentre of the main shock, and that there is a region of lesser seismic activity about 20 km to the east of the main shock.

The HDC analysis provides useful constraints on relative location, but the absolute location of the cluster hypocentre, which controls the absolute locations of all the cluster events, is biased by the deviation of the traveltimes along the actual ray paths from the average global traveltimes model (ak135) used for relocation. The bias in location and origin time depends on the particular distribution of stations and phases in a cluster and is not predictable or consistent across a region. Therefore, each cluster must be calibrated individually if unbiased estimates of absolute location are to be obtained.

For Changureh, we were fortunate to obtain phase arrival time readings from an aftershock network operated by the Iranian Institute of Earthquake Engineering and Seismology (IIEES) (A. M. Farahbod, personal communication, IIEES, Tehran), for a magnitude 4.3 event on 2002 July 3 (event number 12 on Table 1). We used the program HYPOSAT (Schweitzer 2001) to relocate this event with a crustal model for Changureh, derived from the IIEES aftershock data (A. M. Farahbod, personal communication, IIEES, Tehran).

The crustal model features a 7 km thick layer of sediments with $V_p = 5.0 \text{ km s}^{-1}$, underlain by another 7 km thick layer with $V_p = 5.9 \text{ km s}^{-1}$. Shear velocities were derived from $V_p/V_s = 1.74$, also constrained by the aftershock data. Deeper layers of the model are not relevant, because the rays sample only these two layers.

Our analysis of the aftershock data for event 12 revealed one reading that was a clear outlier. The final location was made with 12 P_g readings of stations at distances of between about 5 and 35 km from the event, with an open azimuth of 91° . The RMS residual is 0.216 s. The solution is:

source time: 2002.07.03 19:24:39.2 \pm 0.16 s
 epicentre latitude: $35.731 \pm 0.013^\circ$
 epicentre longitude: $49.026 \pm 0.014^\circ$
 source depth: $7.38 \pm 2.67 \text{ km}$

where the uncertainties are at the 95 per cent confidence level. The depth places the event just below the sediment layer of the local

crustal model determined from the Changureh aftershock data (A. M. Farahbod, personal communication, IIEES, Tehran).

We calibrate the absolute location of the Changureh cluster earthquakes by shifting the cluster in space and time so that the location of the 2002.07.03 event (event number 12) matches the hypocentre determined with the aftershock network data. This requires a shift of the cluster by 17.3 km at an azimuth of 78° , and a shift of -2.55 s in origin time. The calibrated origin times and epicentres are listed in Table 1. It is unlikely that any rotation of the cluster is needed, as such an effect would only arise from very large velocity variations within the dimensions of the cluster. As the dimensions of our cluster are relatively small (events within $\sim 30 \text{ km}$ of the Changureh main shock), we assume that this effect is negligible.

Although this process helps remove bias from our locations, the uncertainty in the absolute locations in Table 1 is still larger than we would wish because of the uncertainty in the location of event 12 in the HDC analysis. The solution, of course, is to find additional data to tie event 12 in more accurately to the rest of the cluster events, or to obtain additional local network solutions for events in our teleseismic cluster. Because of the consistency of the location of event 12 with the bulk of other aftershocks (e.g. Fig. 2), we believe that the calibration process can be trusted to the extent that comparison of these locations with geological and remote sensing observations is warranted.

3.3 Source parameters from seismology

We used long-period body waveforms to constrain the source parameters of the Changureh earthquake. Broad-band digital records from the Global Digital Seismograph Network (GDSN) were obtained from the Incorporated Research Institutions for Seismology (IRIS) data centre, and convolved with a filter that reproduces the bandwidth of the WWSSN 15–100 s long-period instruments. We then used the MT5 version (Zwick *et al.* 1995) of the algorithm of McCaffrey & Abers (1988) and McCaffrey *et al.* (1991) to invert the P and SH waveform data to obtain the strike, dip, rake, centroid depth, seismic moment and source–time function. We always constrained the source to be a double-couple. Details of the now routine procedure we followed can be found in earlier publications (e.g. Berberian *et al.* 2001).

The result of our best-fitting inversion for the main shock is shown in Table 2 along with source parameter estimates from the USGS and Harvard CMT solutions. The fault plane solution and waveforms are shown in Fig. 6. Our solution shows almost pure thrust motion, with a strike of between $\sim 280^\circ$ and 300° on both nodal planes. The centroid depth is $10 \pm 3 \text{ km}$. In Sections 3.4 and 4, we use observations of surface faulting and the geomorphology of the epicentral region to identify the south-dipping nodal plane as the probable fault plane.

3.4 Surface ruptures

Field investigations undertaken shortly after the earthquake by the Geological Survey of Iran (GSI) and the IIEES

Table 2. Source parameters of the 2002 June 22 Changureh earthquake. Strike, dip and rake are given for both nodal planes. We suspect that the southward-dipping nodal plane 2 is the fault plane (see text for full discussion). SV is the slip vector azimuth assuming that the southward-dipping nodal plane is the fault plane. Seismic moment (M_0) is in units of $\times 10^{18} \text{ N m}$.

Date	Time (GMT)	Str 1	Dip 1	Rake 1	Str 2	Dip 2	Rake 2	SV	Depth	M_0	M_w	Source
2002.06.22	02:58:20.1	283	42	77	120	49	101	13	10	5.6	6.4	Body wave inversion
		295	29	99	105	61	85	25	15	6.97	6.5	Harvard CMT
		280	39	76	118	52	101	10	5	6.9	6.5	USGS

(http://www.iiees.ac.ir/English/avaj_report.html) identified a zone (~3 km long) of discontinuous surface ruptures trending ~northwest–southeast near the village of Abdarreah (Fig. 3). In 2003 September we observed the surface breaks at Abdarreah village, where the ruptures appear to follow gently southward-dipping bedding in Neogene marls (Fig. 4a), up to the south with an average slip of ~10 cm, and a maximum slip of only 16 cm. According to IIEES (http://www.iiees.ac.ir/English/avaj_report.html), further discontinuous fractures were found during fieldwork in 2002 from late June to late August. These ruptures were traced for ~14 km trending northwest and southeast from Abdarreah with a maximum offset of 65 cm. The seismological analysis, discussed in Section 4.2, requires fault offsets of 75 cm to 1.5 m, which are larger than the observed ruptures (typically with only ~10 cm of slip at the surface). It is quite common for surface ruptures developed in thrust earthquakes not to be directly related to the seismogenic fault slip, but instead to be related to co-seismic fold growth. In later sections, we discuss the likely origin of these Changureh earthquake ruptures.

4 THE ABDARREH THRUST FAULT: LONG-TERM UPLIFT AND FOLDING

In this section, we demonstrate that a south-dipping thrust fault can be inferred to underlie the epicentral region, based on the pattern of surface uplift and folding. Although the active folding is partially masked by remnants of a pre-existing Neogene topography, diagnostic features can be seen in the incision and disruption of drainage systems.

4.1 Geomorphological indicators of folding at Changureh

The topography in the Khar river valley is generally subdued, dominated by isolated low hills composed of steeply dipping and folded

Neogene marls and red beds that outcrop in places as flat-topped outliers (Figs 3 and 7; Blourchi & Hajian 1979).

Fig. 7(a) shows ~90 m pixel size SRTM (shuttle-borne radar topography mission) digital topography of the Changureh region. Earthquake ruptures mapped to the south of Abdarreah are marked by a black line. Looking in detail at the landscape around the ruptures, we identify a region of slightly elevated topography and extensive fluvial erosion trending ~300° (this region is enclosed by a dashed line and thrust fault symbol in Fig. 7b). We interpret the fluvial incision as a result of surface uplift and folding and refer to this region as the Abdarreah fold. The Abdarreah fold is at least 15 km long (marked on Fig. 3 with black arrows), and may continue further to the southeast along a prominent ridge in Neogene deposits (see Figs 2 and 3). In the absence of definite surface ruptures we cannot be sure whether this apparent southeastward continuation relates to active faulting. The southern limb of the Abdarreah fold is covered in places by Quaternary alluvium (Fig. 7b) and dips gently where it is visible (see also Fig. 9). In contrast, the northern fold limb is represented by a sharp limit to the elevated topography and river incision (Fig. 8). Fig. 8(b) is a photograph looking at this sharp northern margin.

Profiles drawn perpendicular to the fold on SRTM digital topography are shown in Fig. 9. A height difference of ~100 m can be seen across the fold in all profiles. However, this relief is much more difficult to see in map view. This is due partly to the masking effects of the relict Neogene topography (the effect of this topography can be seen in section E–F of Fig. 9). It is also partly due to the soft sediments in which the fold is developed, which have been stripped away, leaving a region of badland erosion and a drainage divide that has retreated to the southwest of the fold axis (Fig. 8a).

The change in height across the Abdarreah fold presumably results from hanging-wall uplift above a southward-dipping thrust fault. Fault-driven uplift and folding can cause the abandonment

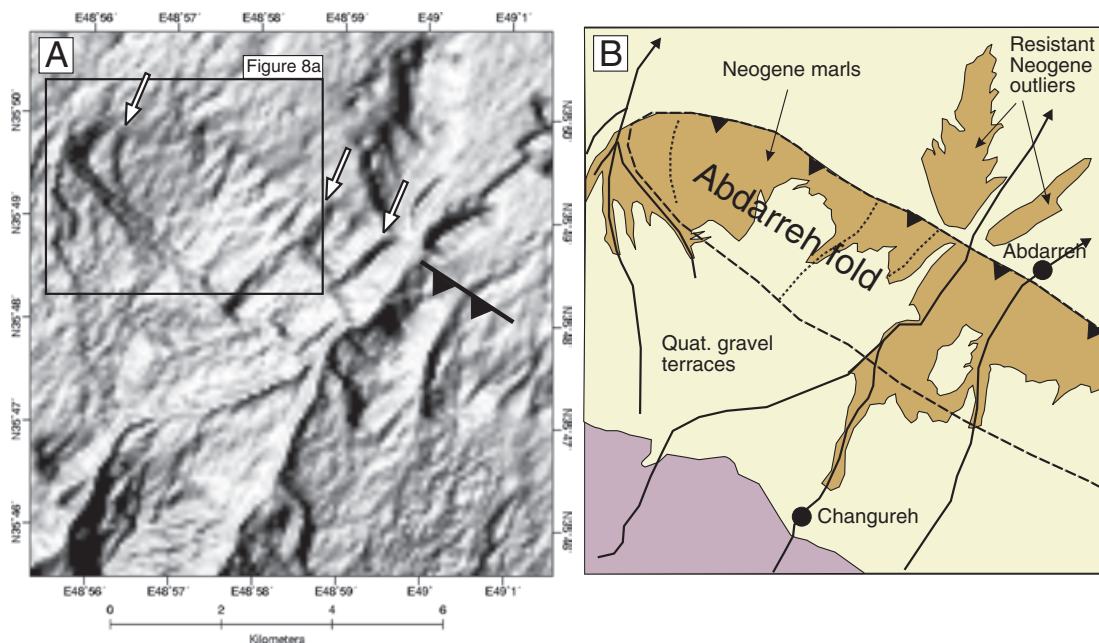


Figure 7. (a) SRTM digital elevation model of the western Abdarreah fold (see Fig. 3 for location). Rivers draining northeast from Kuh-e-Yumer Qezel incise through Quaternary terraces to the south of the fold. At the northern margin of the fold, river incision ceases abruptly. White arrows mark the positions of three linear depressions through the fold. These may represent old, abandoned river channels. The black line represents surface ruptures mapped after the 2002 Changureh earthquake. The box marks the area represented in Fig. 8(a). (b) Geomorphological sketch of Fig. 7(a). The Abdarreah fold, enclosed by the thrust symbol in the north and the dashed line in the south, is growing through Quaternary gravels causing river incision and exposure of underlying Neogene marls. Dotted lines represent possible abandoned river channels identified from the digital topography.

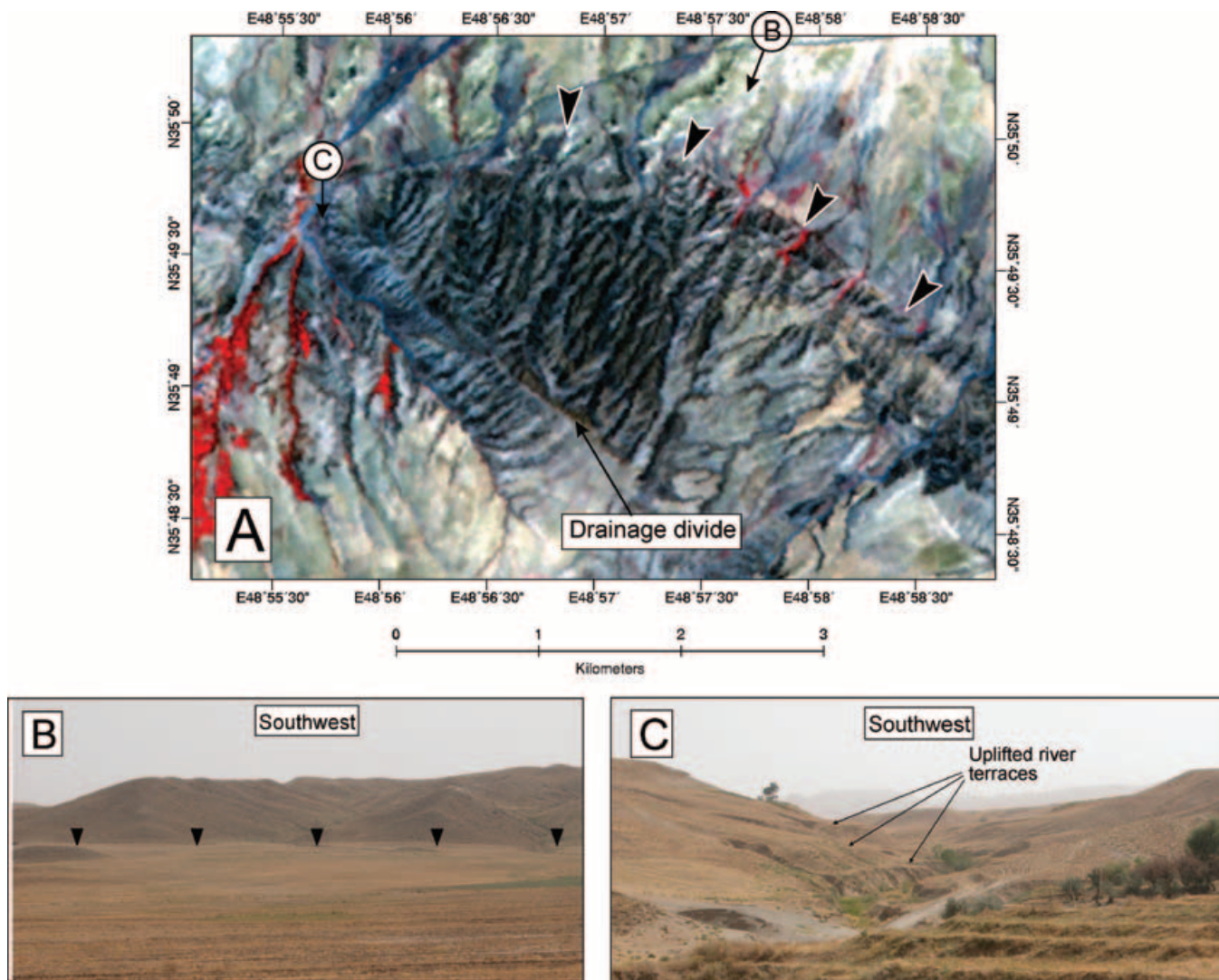


Figure 8. (a) ASTER image (RGB 3n,2,1) of the western nose of the Abdarreh fold (see Fig. 7 for location). Rapid erosion of soft Quaternary gravels and underlying Neogene marls in the core of the fold has caused the drainage divide to retreat towards the southern fold margin. Black arrows mark the sharp northern margin of the fold. (b) Photograph looking 200° from the main road at $35^\circ50'21''\text{N}$, $48^\circ57'40''\text{E}$, at the sharp northern margin of the Abdarreh fold (see Fig. 8a for location). The break in slope is marked by black arrows. (c) Photograph looking south from the main road at $35^\circ49'44''\text{N}$, $48^\circ55'35''\text{E}$, at a series of uplifted and abandoned river terraces in the western nose of the Abdarreh fold (see Fig. 8a for location).

and incision of river channels and alluvial fans (e.g. Benedetti *et al.* 2000; Walker *et al.* 2003). In the region south of the Abdarreh fold (Fig. 10), the streams are actively incising, leaving a sequence of abandoned river terraces that can be observed in the field (Figs 10b–d). However, the widespread river incision ceases abruptly at the northern margin of the Abdarreh fold (Figs 3, 7 and 8). Numerical models of landscape evolution that have analysed the effect of hangingwall uplift above a dipping fault (e.g. Champel *et al.* 2002) also suggest that hangingwall uplift is a major control on the morphology of deforming regions.

In regions of active folding, the rivers cannot always incise quickly enough to keep pace with rapid uplift. This often leads to the defeat and subsequent diversion of river channels around the end of the growing structure (e.g. Jackson *et al.* 1996; Keller *et al.* 1998, 1999; Berberian *et al.* 2000). In such cases, the growth of folds during repeated earthquakes may be inferred from remnants of abandoned and uplifted river channels identified in satellite imagery and digital topography. Three linear northeast–southwest depressions are

identified in Fig. 7(a) (marked by white arrows). These linear features are drawn as dotted lines on Fig. 7(b). The orientation of the linear depressions, and their apparent continuity with rivers to the south of the fold (Fig. 7), lead us to interpret them as abandoned drainage channels (termed ‘dry valleys’ or ‘wind gaps’). In Fig. 11 we show a possible evolution of drainage to the present-day configuration. Fig. 11(a) is an initial state, with a series of northeast-flowing rivers (labelled 1 to 4) crossing the northwest–southeast Abdarreh fold. Continued uplift and folding (presumably during repeated earthquake events) results in the defeat of stream 2, which diverts eastward to join with stream 1, and abandons its original channel through the fold which is preserved as a ‘dry valley’. The combined catchments of streams 1 and 2 presumably provide sufficient power for the river incision to keep pace with the rate of fold uplift. As the underlying thrust fault accumulates displacement, it must also increase in length (e.g. Cowie & Scholz 1992). Westward lateral growth (represented by a large black arrow in Fig. 11a) may be the cause of the apparent westward deflection of streams 3 and 4

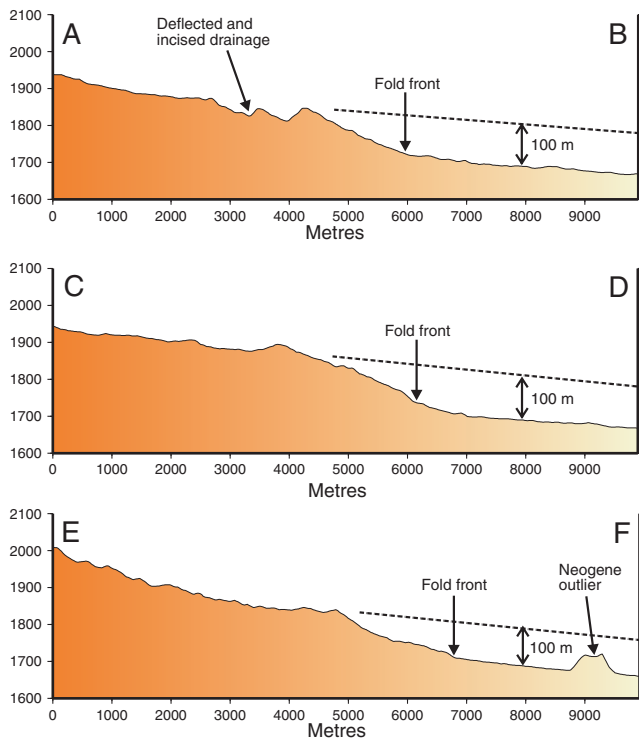


Figure 9. Northeast–southwest topographic profiles across the Abdarreth fold (see Fig. 3b for locations). In each case, the northeast-directed regional slope is offset vertically by ~ 100 m. Section A–B picks out the incised channels of rivers deflected around the western nose of the fold (see Fig. 7). Section E–F demonstrates the effect of outliers of resistant Neogene topography in disguising the Quaternary offsets.

(Fig. 11b). As it crosses the Abdarreth fold, stream 4 has cut down through its bed leaving a series of river terraces (Fig. 8c), presumably as a result of continued northwestward lateral propagation of uplift and folding.

4.2 Relationship between deformation at the surface and fault slip at depth

The southwest-dipping blind thrust fault that we infer to be responsible for the uplift and incision between Abdarreth and Changureh has an orientation and character consistent with the earthquake source parameters determined from seismology (see Table 2). The relocated epicentre of the main shock is situated ~ 10 km to the southwest of the inferred continuation of the Abdarreth fold under a ridge in Neogene deposits (Table 1 and Fig. 2), and suggests both a northwestward and upward rupture propagation. The epicentre is also located ~ 25 km to the southeast of Changureh and Abdarreth villages, where the maximum damage occurred, indicating that damage is focused in the direction of rupture propagation. Given the centroid depth of ~ 10 km and the southward dip of $\sim 49^\circ$ determined from body-waveform modelling (Fig. 6 and Table 1), slip on the southward-dipping nodal plane would project to the surface less than 2 km from the trace of the Abdarreth fold (if the fault is planar, and extends to ~ 13 km depth, as implied by the scaling arguments introduced later in this section). Aftershocks of the Changureh earthquake (see Table 1 and Fig. 2) occur mainly to the northwest of the epicentre of the main shock epicentre and in a region 10–15 km south of the Abdarreth fold, and are therefore presumably the result

of deformation within the hangingwall of a southward-dipping fault. Co-seismic slip on a southward-dipping fault beneath the Abdarreth fold, and projecting to the surface at Abdarreth, would also be consistent with the macroseismic effects, with the most extensive damage occurring at the villages of Abdarreth and Changureh, the latter of which would have been directly above the main rupture (Fig. 3).

In many continental thrust earthquakes, the faulting does not propagate to the surface (e.g. Stein & Yeats 1989). Ruptures generated by earthquakes on these ‘blind’ thrust faults are often surficial secondary ruptures related to fold growth (e.g. Berberian 1979a; Yielding *et al.* 1981; Walker *et al.* 2003; Parsons *et al.* 2004). Small-offset secondary thrust faults in near-surface sediments are often observed within the limbs of growing anticlines (e.g. Oskin *et al.* 2000; Walker & Jackson 2002). Therefore, although the south-dipping surface ruptures described in Section 3.4 are consistent with the source parameters given in Table 2, and suggest that the main rupture may have just reached the surface in this case, the ruptures may instead be surficial structures related to co-seismic folding.

The source–time function in Fig. 6 indicates that the earthquake rupture lasted for ~ 5 s. At a typical rupture velocity of ~ 3 km s^{-1} , the fault length would be ~ 15 km. This is similar to the ~ 15 km total length of the fold identified in the geomorphology (see Fig. 3), although the location of the epicentre of the main shock suggests that the total rupture length may have been ~ 25 – 30 km (Fig. 2). We can use the rupture length to estimate the average amount of slip on the fault plane by assuming that the ratio of slip to rupture length (\bar{u}/L) is 5×10^{-5} , which is typical for intraplate earthquakes (e.g. Scholz 1982; Scholz *et al.* 1986). The average slip calculated using this method is ~ 0.75 – 1.5 m (assuming a rupture length of 15–30 km), which is somewhat more than the ~ 10 cm of displacement we observed at the surface (see Section 3.4). Therefore, even if some of the main rupture did propagate to the surface, the major part of the slip probably did not, and was presumably accommodated by folding at the surface instead. We can also use our estimates of the average slip (~ 1 m), fault length (~ 20 km) and moment (5.6×10^{18} N m) to estimate a down-dip fault width of ~ 9 km. With a centroid depth of ~ 10 km and a fault-plane dip of $\sim 49^\circ$, the main slip event would have occurred over a depth range of ~ 7 – 13 km. These scaling arguments again suggest that the main slip probably failed to reach the surface.

5 DISCUSSION AND CONCLUSIONS

The 2002 June 22 Changureh earthquake occurred on a southward-dipping and partially blind thrust fault that projects to the surface ~ 5 – 10 km north of the Avaj fault along a northwest–southeast-trending fold (the Abdarreth fold). The Changureh earthquake highlights the continued hazard posed by concealed thrust faults in regions of active continental deformation. Concealed thrust faults (i.e. faults that are not directly expressed at the surface, either due to their being blind or due to rapid erosion and sedimentation in the active region) are known to be responsible for many other recent earthquakes within Iran, for example the 1978 Tabas earthquake (e.g. Berberian 1979b; Walker *et al.* 2003), and the Sefidabeh earthquake sequence in 1994 (Berberian *et al.* 2000; Parsons *et al.* 2005).

Our conclusion is that in regions where blind (or partially blind) faults are present, the cumulative surface deformation from many repeated earthquakes will leave features diagnostic of active faulting in the landscape, such as the diversion or abandonment of river channels, abrupt changes from river incision to deposition and abandoned terrace surfaces that can be identified in satellite imagery and

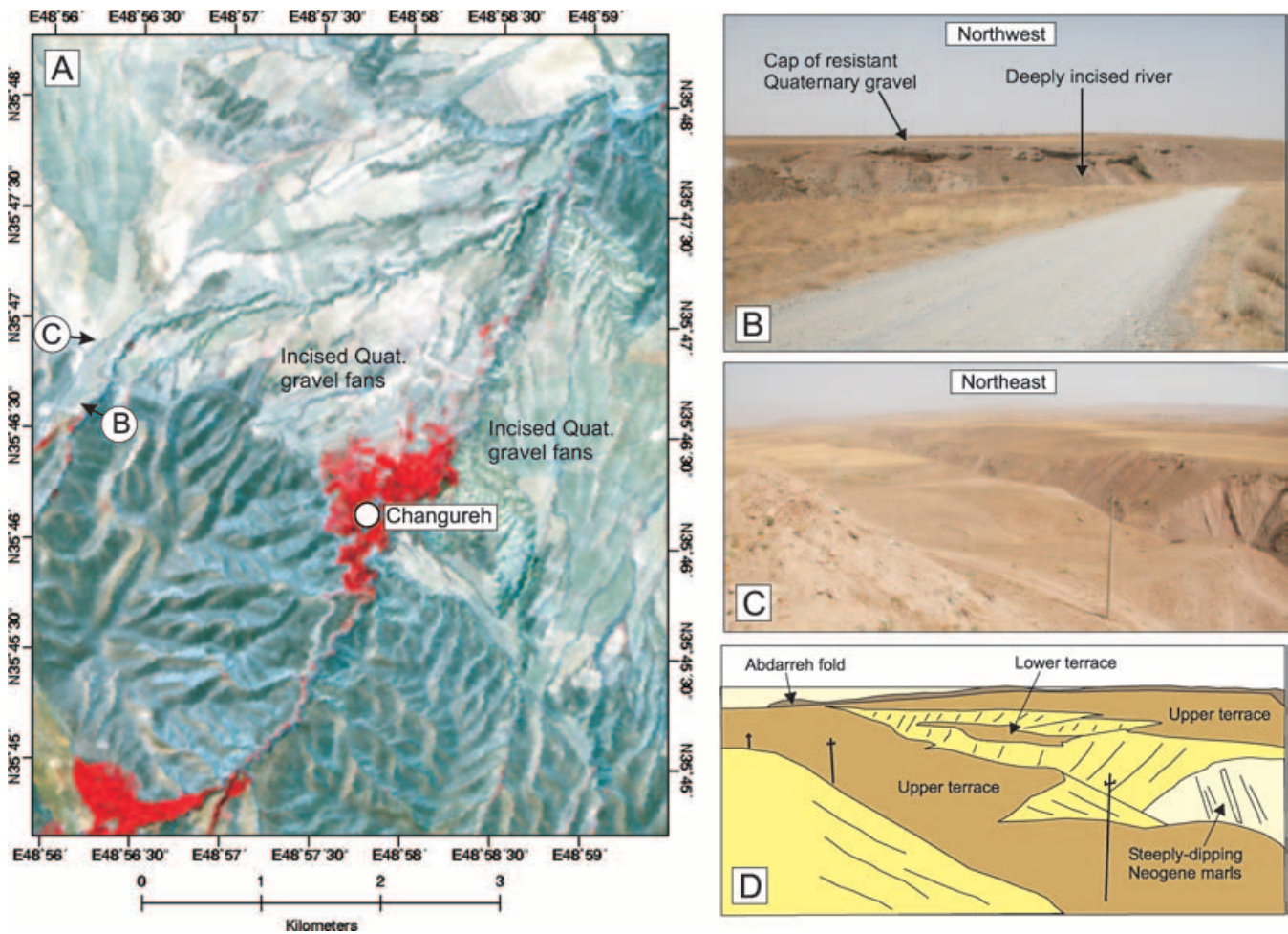


Figure 10. (a) ASTER image of the region to the south of the Abdarreh fold around Changureh village (see Fig. 3 for location). (b) Photograph looking north from 35°46'44"N, 48°56'22"E at gravel river terraces cut through and abandoned by river incision. See part (a) for location. (c) View looking ENE from 35°47'02"N, 48°56'28"E at extensive Quaternary gravel surfaces. See Fig. 10a for location. (d) Sketch of part (c) highlighting the important features of the photograph. Two main terrace levels are preserved in the river cutting. The terraces cover steeply dipping Neogene marls. The Abdarreh fold can be seen in the far distance. Note telegraph poles for scale.

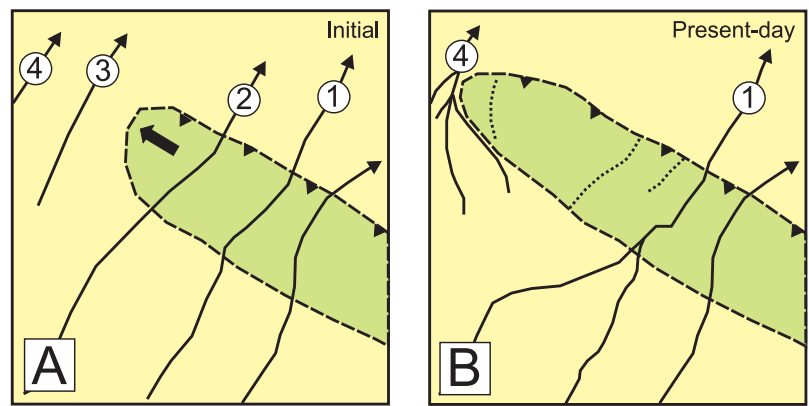


Figure 11. Diagrams showing a possible evolution of the drainage patterns seen in Fig. 7. (a) The initial stage: growth of the northwest-southeast-trending Abdarreh fold interrupts a series of northeast-flowing rivers (labelled 1 to 4). As it accumulates displacement, the fold will grow laterally (represented by a large black arrow). (b) Continued fold growth causes defeat of stream 2, which coalesces with stream 1. The apparent westward deflection of streams 3 and 4 may have been caused by a westward lateral growth of the Abdarreh fold.

the field. Co-seismic anticlinal folding has been observed in blind thrust fault earthquakes (e.g. Stein & Yeats 1989), and can now be imaged using InSAR (for example the 1994 Sefidabeh earthquake sequence, Parsons *et al.* 2005). However, the cumulative folding

from many repeated earthquakes is not always as easy to observe in the geomorphology of active regions, primarily due to the masking effect of pre-existing topography. This is the case at Changureh, where the growing Abdarreh fold is superimposed on relict

Neogene topography. The blind fault responsible for the 1994 Sefidabeh earthquake sequence in eastern Iran is also hard to see in the topography, in this case because the fold is growing under a ridge of resistant volcanic rock (Berberian *et al.* 2000; Parsons *et al.* 2005). In the Sefidabeh example, it is again the disruption to drainage systems that provide the best evidence of anticlinal uplift (Berberian *et al.* 2000).

ACKNOWLEDGMENTS

We would like to thank the Geological Survey of Iran in Tehran for their continued support of our work and for enabling us to visit the region in 2003. We thank E. R. Engdahl for his help with the relocation analysis, A. M. Farahbod for providing us with data from the IIEES local network and L. A. Ramsey for help with ESRI software. Sebastien Carretier, Rowena Lohman and Roger Clark are thanked for their helpful reviews. RTW thanks D. McKenzie and the Royal Society for financial support. This work was supported by the NERC Centre for the Observation and Modelling of Earthquakes and Tectonics (COMET). This is Cambridge Earth Science Contribution No ES 7760.

REFERENCES

- Ambraseys, N.N., 1963. The Buyin-Zara (Iran) earthquake of September, 1962: a field report, *Bull. seism. Soc. Am.*, **53**, 705–740.
- Ambraseys, N.N., 2001. Reassessment of earthquakes, 1900–1999, in the Eastern Mediterranean and the Middle East, *Geophys. J. Int.*, **145**, 471–485.
- Ambraseys, N.N. & Melville, C.P., 1982. *A History of Persian Earthquakes*, Cambridge University Press, Cambridge.
- Benedetti, L., Tapponnier, P., King, G.C.P., Meyer, B. & Manighetti, I., 2000. Growth folding and active thrusting in the Montello region, northern Italy, *J. geophys. Res.*, **105**, 739–766.
- Berberian, M., 1976. *Contribution to the Seismotectonics of Iran (Part II)*, Report No 39, Geological Survey of Iran, Tehran.
- Berberian, M., 1979a. Earthquake faulting and bedding thrust associated with the Tabas-e-Golshan (Iran) earthquake of September 16, 1978, *Bull. seism. Soc. Am.*, **69**, 1861–1887.
- Berberian, M., 1979b. Evaluation of instrumental and relocated epicentres of Iranian earthquakes, *Geophys. J. R. astr. Soc.*, **58**, 625–630.
- Berberian, M. & Yeats, R. S., 1999. Patterns of historical earthquake rupture in the Iranian plateau, *Bull. seism. Soc. Am.*, **89**, 120–139.
- Berberian, M., Jackson, J.A., Qorashi, M., Talebian, M., Khatib, M.M. & Priestley, K., 2000. The 1994 Sefidabeh earthquakes in eastern Iran: blind thrusting and bedding-plane slip on a growing anticline, and active tectonics of the Sistan suture zone, *Geophys. J. Int.*, **142**, 283–299.
- Berberian, M. *et al.*, 2001. The March 14 1998 Fandoqa earthquake (M_w 6.6) in Kerman province, SE Iran: re-rupture of the 1981 Sirch earthquake fault, triggering of slip on adjacent thrusts, and the active tectonics of the Gowk fault zone, *Geophys. J. Int.*, **146**, 371–398.
- Blourchi, M.H. & Hajian, J., 1979. *Geological Quadrangle Map of Iran No D5 (Kabudar Ahang Sheet)*, Scale 1:250,000, Geological Survey of Iran, Tehran.
- Bondar, I., Myers, S.C., Engdahl, E.R. & Bergman, E.A., 2004. Epicentre accuracy based on seismic network criteria, *Geophys. J. Int.*, **156**, 1–14, doi:10.1046/j.1365-246X.2004.02070.x
- Champel, B., van der Beek, P., Mugnier, J.-L. & Leturmy, P., 2002. Growth and lateral propagation of fault-related folds in the Siwaliks of western Nepal: rates, mechanisms, and geomorphic signature, *J. geophys. Res.*, **107**(B6), doi:10.1029/2001JB000578.
- Cowie, P.A. & Scholz, C.H., 1992. Growth of faults by accumulation of seismic slip, *J. geophys. Res.*, **97**, 11 085–11 095.
- Engdahl, E.R., van der Hilst, R. & Buland, R., 1998. Global teleseismic earthquake relocation with improved travel times and procedures for depth determination, *Bull. seism. Soc. Am.*, **88**, 722–743.
- Jackson, J., 2001. Living with earthquakes: know your faults, *J. Earthquake Eng.*, **5** (Special Issue 1), 5–123.
- Jackson, J., Norris, R. & Youngson, J., 1996. The structural evolution of active fault and fold systems in central Otago, New Zealand: evidence revealed by drainage patterns, *J. Struct. Geol.*, **18**, 217–234.
- Jackson, J., Priestly, K., Allen, M. & Berberian, M., 2002. Active tectonics of the South Caspian basin, *Geophys. J. Int.*, **148**, 214–245.
- Jordan, T.H. & Sverdrup, K.A., 1981. Teleseismic location techniques and their application to earthquake clusters in the south-central Pacific, *Bull. seism. Soc. Am.*, **71**, 1105–1130.
- Keller, E.A., Zepeda, R.L., Rockwell, T.K., Ku, T.L. & Dinklage, W.S., 1998. Active tectonics at Wheeler Ridge, southern San Joaquin Valley, California, *Geol. Soc. Am. Bull.*, **110**, 298–310.
- Keller, E.A., Gurrrola, L. & Tierney, T.E., 1999. Geomorphic criteria to determine direction of lateral propagation of reverse faulting and folding, *Geology*, **27**, 515–518.
- Matheson, S.A., 1976. *Persia: an Archaeological Guide*, 2nd edn, Faber & Faber, London.
- McCaffrey, R. & Abers, G., 1988. *SYN3: a Program for Inversion of Teleseismic Body Waveforms on Microcomputers*, Airforce Geophysical Laboratory Technical Report AFGL-TR-88-0099, Hanscomb Air Force Base, MA.
- McCaffrey, R., Zwick, P. & Abers, G., 1991. *SYN4 Program*, IASPEI Software Library, Vol. 3, pp. 81–166.
- McClusky, S. *et al.*, 2000. Global Positioning System constraints on plate kinematics and dynamics in the eastern Mediterranean and Caucasus, *J. geophys. Res.*, **105**, 5695–5719.
- Meyer, B., Tapponnier, P., Bourjot, L., Metivier, F., Gaudemar, Y., Peltzer, G., Shunmin, G. & Zhitai, C., 1998. Crustal thickening in Gansu-Qinghai, lithospheric mantle subduction, and oblique, strike-slip controlled growth of the Tibet plateau, *Geophys. J. Int.*, **135**, 1–47.
- Mori, J., Wald, D.J. & Wesson, R.L., 1995. Overlapping fault of the 1971 San Fernando and 1994 Northridge, California earthquakes, *Geophys. Res. Lett.*, **22**(9), 1033–1036.
- Oskin, M., Sieh, K., Rockwell, T., Miller, G., Gupta, P., Curtis, M., McArdle, S. & Elliot, P., 2000. Active parasitic folds on the Elysian Park anticline: implications for seismic hazard in central Los Angeles, California, *Geol. Soc. Am. Bull.*, **112**, 693–707.
- Parsons, B., Wright, T., Rowe, P., Andrews, J., Jackson, J., Walker, R., Khatib, M. & Talebian, M., 2005. The Sefidabeh earthquakes revisited: an example of a growing fold, *Geophys. J. Int.*, submitted.
- Ritzwoller, M.H., Shapiro, N.M., Levshin, A.L., Bergman, E.A. & Engdahl, E.R., 2003. Ability of a global three-dimensional model to locate regional events, *J. geophys. Res.*, **108**(B7), 2353, doi:10.1029/2002JB002167.
- Scholz, C., 1982. Scaling laws for large earthquakes: consequences for physical models, *Bull. seism. Soc. Am.*, **72**, 1–14.
- Scholz, C.H., Aviles, C. & Wesnousky, S., 1986. Scaling differences between large intraplate and interplate earthquakes, *Bull. seism. Soc. Am.*, **76**, 65–70.
- Schweitzer, J., 2001. HYPOSAT—an enhanced routine to locate seismic events, *Pure appl. Geophys.*, **158**, 277–289.
- Sella, G.F., Dixon, T.H. & Mao, A., 2002. REVEL: a model for recent plate velocities from space geodesy, *J. geophys. Res.*, **107**, doi:10.1029/2000JB000033.
- Shearer P. M., 2002. Parallel fault strands at 9-km depth resolved on the Imperial Fault, southern California, *Geophys. Res. Lett.*, **29**(14), doi:10.1029/2002GL015302.
- Stein, R. & Yeats, R.S., 1989. Hidden earthquakes, *Sci. Am.*, **260**, 48–57.
- Tatar, M., Hatzfeld, D., Martinod, J., Walpersdorf, A., Ghafori-Ashtiany, M. & Chery, J., 2003. The present-day deformation of the central Zagros from GPS measurements, *Geophys. Res. Lett.*, **29**, 1927–1930.
- Vernant, Ph. *et al.*, 2004. Contemporary crustal deformation and plate kinematics in Middle East constrained by GPS measurements in Iran and northern Oman, *Geophys. J. Int.*, **157**, 381–398.

- Waldhouser, F. & Ellsworth, W.L., 2000. A double-difference earthquake location algorithm: method and application to the northern Hayward fault, California, *Bull. seism. Soc. Am.*, **90**, 1353–1368.
- Walker, R. & Jackson, J., 2002. Offset and evolution of the Gowk fault, S.E. Iran: a major intra-continental strike-slip system, *J. Struct. Geol.*, **24**, 1677–1698.
- Walker, R., Jackson, J. & Baker, C., 2003. Thrust faulting in eastern Iran: source parameters and surface deformation of the 1978 Tabas and 1968 Ferdows earthquake sequences, *Geophys. J. Int.*, **152**, 749–765.
- Yielding, G., Jackson, J.A., King, G.C.P., Sinval, H., Vita-Finzi, C. & Wood, R.M., 1981. Relations between surface deformation, fault geometry, seismicity, and rupture characteristics during the El Asnam (Algeria) earthquake of 10 October 1980, *Earth planet. Sci. Lett.*, **56**, 287–304.
- Zhou, H.-W., 1994. Rapid three-dimensional hypocentral determination using a master station method, *J. Geophys. Res.*, **99**(B8), 15 439–15 456, doi:10.1029/94JB00934.
- Zwick, P., McCaffrey, R. & Abers, G., 1995. *MT5 Program*, IASPEI Software Library, Vol. 4.